MRI Contrast Agents

[Gd(AAZTA)]$^-$ Derivatives with *n*-Alkyl Acid Side Chains Show Improved Properties for their Application as MRI Contrast Agents**

Flávio Vinicius Crizóstomo Kock,[a, b] Attila Forgács,[c, d] Nicol Guidolin,[e] Rachele Stefania,[b] Adrienn Vágner,[c] Eliana Gianolio,*[b] Silvio Aime,[b] and Zsolt Baranyai*[e]

Abstract: Herein, the synthesis and an extensive characterization of two novel Gd(AAZTA) (AAZTA = 6-amino-6-methylperhydro-1,4-diazepine tetra acetic acid) derivatives functionalized with short (C_2 and C_4) *n*-alkyl acid functions are reported. The carboxylate functionality is the site for further conjugations for the design of more specific contrast agents (CAs). Interestingly, it has been found that the synthesized complexes display enhanced properties for use as MRI contrast agents on their own. The stability constants determined by using potentiometric titration and UV/Vis spectrophotometry were slightly higher than the one reported for the parent Gd(AAZTA) complex. This observation might be accounted for by the larger sigma-electron donation of the acyl substituents with respect to the one provided by the methyl group in the parent complex. As far as concerns the kinetic stability, transmetallation experiments with endogenous ions (e.g., Cu^{2+}, Zn^{2+} and Ca^{2+}) implied that the Gd^{3+} ions present in these Gd(AAZTA) derivatives show somewhat smaller susceptibility to chemical exchange towards these ions at 25 °C, close to the physiological condition. The ^{1}H NMR spectra of the complexes with Eu^{III} and Yb^{III} displayed a set of signals consistent with half the number of methylene protons present on each ligand. The number of resonances was invariant over a large range of temperatures, suggesting the occurrence of a fast interconversion between structural isomers. The relaxivity values (298 K, 20 MHz) were consistent with $q = 2$ being equal to 8.8 $mM^{-1}s^{-1}$ for the C_2 derivative and 9.4 $mM^{-1}s^{-1}$ for the C_4 one, that is, sensibly larger than the one reported for Gd(AAZTA) (7.1 $mM^{-1}s^{-1}$). Variable-temperature (VT)-T_2 ^{17}O NMR measurements showed, for both complexes, the presence of two populations of coordinated water molecules, one in fast and one in slow exchange with the bulk water. As the high-resolution ^{1}H NMR spectra of the analogs with Eu^{III} and Yb^{III} did not show the occurrence of distinct isomers (as frequently observed in other macrocyclic lanthanide(III)-containing complexes), we surmised the presence of two fast-interconverting isomers in solution. The analysis of the ^{17}O NMR VT-T_2 profiles versus temperature allowed their relative molar fraction to be established as 35% for the isomer with the fast exchanging water and 65% for the isomer with the water molecules in slower exchange. Finally, ^{1}H NMRD profiles over an extended range of applied magnetic field strengths have been satisfactory fitted on the basis of the occurrence of the two interconverting species.

Introduction

The design of novel contrast agents (CAs) for magnetic resonance imaging (MRI) is still a task of strong interest in the search for safe, rapid, and non-invasive clinical diagnostics.[1] Up to now, CAs have been represented by paramagnetic metal complexes characterized by a high longitudinal paramagnetic relaxivity (r_{1p}). Several paramagnetic ions, among them Mn^{2+},

[a] *F. V. C. Kock*
São Carlos Institute of Chemistry
University of São Paulo
Avenida Trabalhador São Carlense 400, 13566-590, São Paulo (Brazil)
[b] *F. V. C. Kock, R. Stefania, Dr. E. Gianolio, Prof. S. Aime*
Department of Molecular Biotechnologies and Health Science
University of Turin
Via Nizza 52, 10125, Turin (Italy)
E-mail: eliana.gianolio@unito.it
[c] *Dr. A. Forgács, Dr. A. Vágner*
Department of Inorganic and Analytical Chemistry
University of Debrecen
Egyetem tér 1, 4010, Debrecen, (Hungary)
[d] *Dr. A. Forgács*
MTA-DE Redox and Homogeneous Catalytic Reaction Mechanisms Research Group
Egyetem tér 1, Debrecen, 4032 (Hungary)
[e] *N. Guidolin, Dr. Z. Baranyai*
Bracco Imaging SpA
Bracco Research Center
Via Ribes 5, 10010, Colleretto Giacosa (TO) (Italy)
E-mail: zsolt.baranyai@bracco.com

[**] *AAZTA = 6-amino-6-methylperhydro-1,4-diazepine tetra acetic acid.*

Supporting information and the ORCID identification number(s) for the author(s) of this article can be found under: https://doi.org/10.1002/chem.202004479.

Mn^{3+}, Fe^{3+}, and Gd^{3+}, can exert a strong paramagnetic effect on the water proton relaxation, with Gd^{3+} ions being the candidate of choice owing to the high paramagnetism associated with its seven unpaired electrons and the relatively long electron relaxation time.[2–4]

It was immediately evident, in the early days of their consideration as MRI-CAs, that free Gd^{3+} ions could not be administered to living systems because of their antagonistic role with respect to the endogenous Ca^{2+} and Zn^{2+} ions.[3] Therefore, the complexation of Gd^{3+} ions with ligands to yield highly stable chelates has been a fundamental step in the search for new contrast agents. Nowadays, the clinically used Gd^{3+}-based contrast agents (GBCAs)[5] have only one water molecule coordinated ($q=1$) to the paramagnetic ion,[6] in spite of the fact that the relaxivity scales up with the number of coordinated water molecules. This choice relies on the early observation that the coordination with octadentate ligands yields highly stable complexes, which ensure a limited in vivo release of Gd^{3+} ions. However, the search for systems containing two or three coordinated water molecules still endowed with good stability, compatible with their in vivo use, is an area of intense activity.[7,8] In this context, the AAZTA ligand (6-amino-6-methylperhydro-1,4-diazepine tetra acetic acid) (and its derivatives) has been considered as an excellent system for the design of $q=2$ GBCAs (Scheme 1). In fact, high relaxivities were reported for AAZTA chelates forming lipid-based aggregates[9] or able to bind to human serum albumin (HSA).[10] For these applications, bifunctional AAZTA derivatives were designed to embody remote free functional groups ready for the conjugation step with the selected moieties.[11–15] The aim of the herein reported work was to address a detailed physicochemical characterization of two novel Gd(AAZTA) derivatives functionalized with short (C_2 and C_4) spaced acid functions (Scheme 1), designed to be used in further conjugations with a variety of targeting vectors, lipophilic chains, or to form multimeric species.

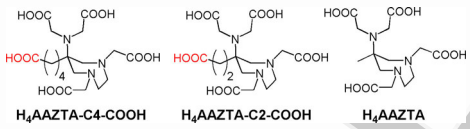

Scheme 1. Structures of H_4AAZTA, H_4AAZTA-C_2-COOH, and H_4AAZTA-C_4-COOH ligands.

Results and Discussion

The H_4AAZTA-C_2-COOH and H_4AAZTA-C_4-COOH ligands are the derivative of H_4AAZTA in which the methyl group is substituted by *n*-propionic and *n*-valeric acid pendants (Scheme 1) for conjugation purposes.[15,16] Generally, three N and four carboxylate O atoms can simultaneously bind the metal ion in the AAZTA complexes.[17–22] The presence of *n*-propionate and *n*-valerate pendants instead of the methyl substituent might affect the equilibrium, kinetic, relaxation, and structural properties of the metal complexes formed with AAZTA-C_2-COO^- and AAZTA-C_4-COO^- ligands. Indeed, the presence of the *n*-valeric acid pendant used for the conjugation of DATA ligand ($DATA^{5m}$) to biologically active molecules evidently influences the physicochemical properties of the Ga^{III} complexes.[13–15] To get more insights into the role the conjugating moieties may have on the physicochemical properties, the behavior of the metal complexes formed with the AAZTA-C_2-COO^- and AAZTA-C_4-COO^- has been investigated close to physiological conditions (0.15 M NaCl, 25 °C).

Synthesis of ligands and their Ln^{III} complexes (Ln = Gd^{3+} and Eu^{3+})

The synthesis route of the ligand H_4AAZTA-C_4-COOH (**5**) is shown in Scheme 2. It was obtained from its bifunctional prochelating agent AAZTA-C_4-(tBu)$_4$ (**4**) after cleavage of all protecting groups with trifluoroacetic acid (TFA). Compound **4** was successfully synthesized over four steps following the protocol described by Manzoni et al.[12] Briefly, compound **1**, a diazepane ring, was formed by a double nitro-Mannich reaction between *N*,*N*′-dibenzylethylenediamine, paraformaldehyde, and 6-nitrohexanoic acid methyl ester in nearly quantitative yield. Hydrogenolysis using palladium on carbon and H_2 removed the benzyl protecting groups at the endocyclic amines and simultaneously reduced the nitro group to an amine. The product was directly reacted with *tert*-butyl bromoacetate to form tetra-alkylated compound **3**. Deprotection of the methyl ester protecting groups were carried out by using 1 M lithium hydroxide and tetrahydrofuran (THF) solution to receive the bifunctional chelator AAZTA-C_4-(tBu)$_4$.

The synthesis route of the ligand H_4AAZTA-C_2-COOH (**5a**) is shown in Scheme 3, it was obtained from its bifunctional prochelating agent AAZTA-C_2-(Me)$_4$ (**4a**) by ester hydrolysis of all protecting groups with lithium hydroxide. Compound **4a** was successfully obtained over five steps, starting from the synthesis of hydroxymethyl diazepine (**1a**) by double nitro-Mannich reaction between *N*,*N*′-dibenzylethylenediamine, paraformaldehyde, and 2-nitroethanol. Then, compound **1a** was reacted with *tert*-butyl acrylate and tBuOK in THF, by tandem retro-Henry and Michael reactions,[16] to afford compound **2a** in good yield. Hydrogenolysis using palladium on carbon and H_2 and subsequent alkylation with methyl bromoacetate yielded the compound **3a**. Deprotection of the *tert*-butyl ester with TFA yielded the bifunctional agent derivative **4a**.

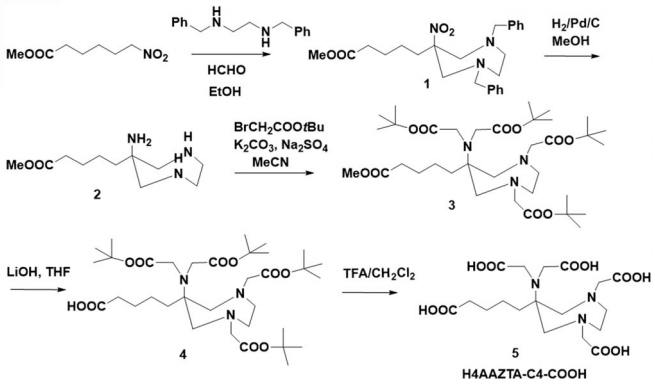

Scheme 2. The synthesis of H_4AAZTA-C_4-COOH.

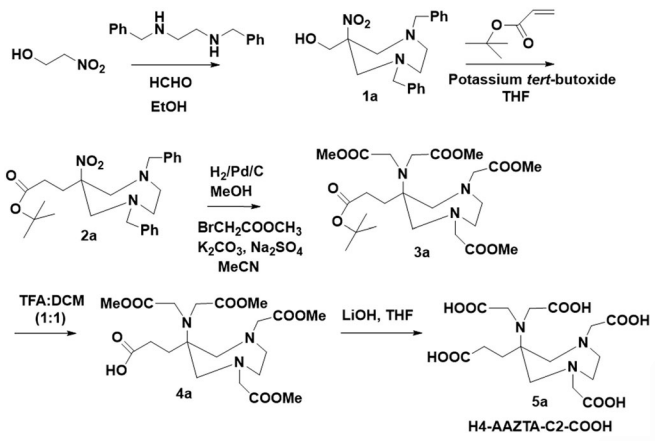

Scheme 3. The synthesis of H_4AAZTA-C_2-COOH.

The Ln^{III} complexes of AAZTA-C_4-COO^- and AAZTA-C_2-COO^- were obtained by the addition of stoichiometric amounts of $EuCl_3$ or $GdCl_3$ to the ligand solution at pH 6.5. The formation of Ln^{III} complexes was confirmed by mass spectrometry.

Solution equilibria of the AAZTA-C_2-COO^- and AAZTA-C_4-COO^- ligands and its complexes

Protonation equilibria of the AAZTA-C_2-COO^- and AAZTA-C_4-COO^- ligands

The protonation constants of the ligand, defined by Equation (1) were determined by pH-potentiometry and the values are listed in Table 1 (standard deviations are shown in parentheses). The charges of the ligands and complexes will be indicated only when they are deemed necessary.

$$K_i^H = \frac{[H_iL]}{[H_{i-1}L][H^+]} \quad (1)$$

where $i = 1, 2, \ldots 7$. The protonation sequence of the AAZTA ligand was already fully characterized by both spectroscopic and potentiometric methods.[18] The first protonation process was shown to occur at the nitrogen atoms of the endo- and exocyclic nitrogen atoms of the ligand backbone (the protonation occurs partially at all nitrogen atoms). The second protonation takes place at the endocyclic nitrogen, whereas the first proton is moved to the exocyclic nitrogen owing to the electrostatic repulsion between the protonated nitrogen atoms. Further protonations occur at the ring carboxylate groups attached to the non-protonated endocyclic nitrogen, the non-protonated endocyclic nitrogen, and/or the carboxylate pendant arms of the exocyclic nitrogen atom, respectively (Scheme S1 in the Supporting Information). According to the similarities to the parent AAZTA, the observed protonation sequence of AAZTA-C_2-COO^- and AAZTA-C_4-COO^- ligands was very similar. A comparison of the protonation constants obtained in the presence of the same background electrolyte (0.15 M NaCl, Table 1) indicated that the $\log K_1^H$ and $\log K_3^H$ values of the AAZTA-C_2-COO^- and AAZTA-C_4-COO^- ligands are slightly larger than the corresponding protonation constants of the parent AAZTA. By taking into account the protonation constant of *n*-propionic acid and *n*-valeric acid (propionic acid: $\log K_1^H = 4.53$, *n*-valeric acid: $\log K_1^H = 4.69$, 1.0 M $NaClO_4$, 25 °C),[23] one can assume that the third protonation of AAZTA-C_2-COO^- and AAZTA-C_4-COO^- occurs at the carboxylate group of the *n*-propionic and the *n*-valeric side chains. The last three protonation constants of AAZTA-C_2-COO^- and AAZTA-C_4-COO^- ($\log K_4^H$, $\log K_5^H$, and $\log K_6^H$) characterizing the protonation of the ring carboxylate and non-protonated exocyclic nitrogen or carboxylate groups, are very similar and comparable with the corresponding $\log K_i^H$ values ($\log K_3^H$, $\log K_4^H$, and $\log K_5^H$) of the AAZTA ligand. The somewhat higher $\log K_1^H$ value of AAZTA-C_2-COO^- and AAZTA-C_4-COO^- might be explained by the electron-donating properties of the *n*-propionic acid and the *n*-valeric side chains, which might influence the basicity of the exo- and endocyclic nitrogen atoms. It is important to note that the $\log K_1^H$ value of AAZTA and its derivative ligands determined in 0.15 M NaCl solution is significantly smaller than the value obtained in 0.1 M KCl or 0.1 M Me_4NCl solutions,[18] which might be explained by the formation of the Na^I complexes, which competes with the first protonation process.

Table 1. Protonation constants of AAZTA, AAZTA-C_2-COOH, and AAZTA-C_4-COOH ligands (25 °C).

i	AAZTA-C_4-COO^- 0.15 M NaCl	AAZTA-C_2-COO^-	AAZTA 0.15 M NaCl[a]	0.1 M KCl[b]
$\log K_1^H$	10.48 (1)	10.22 (1)	10.06	11.23
$\log K_2^H$	6.90 (1)	6.53 (1)	6.50	6.52
$\log K_3^H$	4.68 (1)	4.33 (2)	3.77	3.78
$\log K_4^H$	3.73 (1)	3.62 (1)	2.33	2.24
$\log K_5^H$	2.60 (1)	2.91 (1)	1.51	1.56
$\log K_6^H$	1.80 (2)	2.03 (2)	–	–
$\log K_7^H$	1.09 (3)	1.23 (3)	–	–
$\Sigma \log K_i^H$	31.27/26.59[c]	30.86/26.53[c]	24.16	25.33

[a] Ref. [19]. [b] Ref. [18]. [c] The protonation constant of the propionic acid and the *n*-valeric acid was not considered owing to a negligible role in metal binding.

Complexation properties with $M^{2+/3+}$ cations

The $\Sigma \log K_i^H$ values, presented in Table 1, clearly indicate that the total basicity of the AAZTA-C_2-COO^- and AAZTA-C_4-COO^- is slightly higher than of AAZTA. By taking into account the higher basicity of AAZTA-C_2-COO^- and AAZTA-C_4-COO^-, the stability constants of their Ln^{III} complexes are expected to be somewhat higher than that of the parent AAZTA complex. However, the stability constants of the Ln(AAZTA-C_2-COO^-)$^{2-}$ and Ln(AAZTA-C_4-COO^-)$^{2-}$ complexes might be influenced by the flexibility of the coordination cage through the presence of the side chains.

The stability and protonation constants of the metal complexes formed with the AAZTA-C_2-COO^- and AAZTA-C_4-COO^- ligand are defined by Equations (2) and (3).

$$K_{ML} = \frac{[ML]}{[M][L]} \quad (2)$$

$$K_{MH_iL} = \frac{[MH_iL]}{[MH_{i-1}L][H^+]} \quad (3)$$

where $i = 1, 2, \ldots 4$. The protonation and stability constants of the Ca^{II}, Zn^{II}, and Ln^{III} complexes formed with AAZTA-C_2-COO^- and AAZTA-C_4-COO^- ligands have been calculated from the pH-potentiometric titration curves obtained at 1:1 metal/ligand concentration ratios. The best fitting was obtained by assuming the formation of ML, MHL, MH_2L, MH_3L, and MH_4L species in equilibrium. The formation of the deprotonated $[M(L)H_{-1}]^{n-}$ complexes takes place at pH > 9.0, as indicated by the base consumption in the titration curves (M = Zn^{2+} and Cu^{2+}, $n = 2$; M = Ln^{3+}, $n = 3$). These processes can be interpreted by assuming a hydrolysis of the metal ion, which takes place by the coordination of an OH^- ion with the formation of $[M(L)H_{-1}]^{n-}$ species. The protonation of the $[M(L)H_{-1}]^{n-}$ species is characterized by the equilibrium constant $K_{M(L)H-1}$ [Eq. 4]:

$$K_{M(L)H_{-1}} = \frac{[ML]}{[M(L)H_{-1}][H^+]} \quad (4)$$

The stability and protonation constants of the Ca^{II}, Zn^{II}, Cu^{II}, and Ln^{III} complexes obtained by using pH potentiometric titration and UV/Vis spectrophotometric techniques are presented and compared with those of the corresponding AAZTA complexes in Table 2. The UV/Vis spectrophotometric studies of Cu^{2+}–AAZTA-C_2-COO^- and Cu^{2+}–AAZTA-C_4-COO^- systems are summarized in the Supporting Information. The comparison of the stability constants reported in Table 2 indicates that Ca^{II}, Zn^{II}, and Ln^{III} complexes formed by AAZTA-C_2-COO^- and AAZTA-C_4-COO^- ligands are comparable and slightly higher than those of the corresponding AAZTA complexes owing to the similar basicities of the AAZTA-C_2-COO^-, AAZTA-C_4-COO^-, and AAZTA ligands. Interestingly, the stability constants for the Cu(AAZTA-C_2-COO^-) and Cu(AAZTA-C_4-COO^-) complexes are smaller by 0.6 and 1.6 log$K$ units than that of the parent Cu(AAZTA). Moreover, the stability constant of the Cu(AAZTA-C_4-COO^-) is about 1 log$K$ unit lower than that of the Cu(AAZTA-C_2-COO^-). Based on the distorted octahedral structure of the Cu(AAZTA)$^{2-}$ (Cu^{II} ion is coordinated by the exo- and endocyclic nitrogens and carboxylate oxygen atoms in equatorial positions, whereas the other endocyclic nitrogen and one of the exocyclic carboxylate oxygen atoms are in axial positions),[19] it can be reasonably assumed that the coordination of the more basic exo- and endocyclic nitrogen atoms results in the further distortion of the Cu^{II} complexes,[19] which might cause the slight decrease of the stability constant of the Cu(AAZTA-C_2-COO^-) and Cu(AAZTA-C_4-COO^-) upon the increase of the basicity of the exo- and endocyclic nitrogen atoms.

Table 2. Stability and protonation constants of AAZTA-C_4-COO^-, AAZTA-C_2-COO^-, and AAZTA complexes formed with Ca^{2+}, Mn^{2+}, Zn^{2+}, and Cu^{2+} ions (0.15 M NaCl, 25 °C).

I	AAZTA-C_4-COO^- 0.15 M NaCl	AAZTA-C_2-COO^-	AAZTA 0.15 M NaCl[a]	0.1 M KCl[b]
CaL	12.05 (2)	11.91 (1)	11.75	12.76
CaHL	4.77 (2)	4.36 (1)	3.41	3.34
CaH_2L	3.27 (2)	3.58 (3)	–	–
ZnL	17.05 (3)	16.93 (3)	16.02	18.01
ZnHL	4.74 (3)	4.48 (3)	3.95	3.87
ZnH_2L	3.76 (2)	3.61 (3)	2.53	2.36
ZnH_3L	2.76 (2)	2.74 (3)	–	–
$ZnLH_{-1}$	11.39 (4)	11.44 (5)	11.36	11.25
CuL[c]	18.94 (5)	19.96 (5)	20.60	22.27
CuHL	4.79 (2)	4.54 (3)	3.86	4.00
CuH_2L	3.91 (2)	3.86 (2)	2.43	2.72
CuH_3L	2.88 (2)	2.94 (2)	1.37	–
CuH_4L	1.31 (2)	1.40 (4)	–	–
$CuLH_{-1}$	11.02 (3)	11.23 (2)	10.62	10.81
LaL	17.24 (2)	16.98 (3)	16.48	17.53
LaHL	4.68 (1)	4.36 (1)	1.90	1.97
LaH_2L	2.37 (2)	2.59 (2)	–	–
GdL	20.33 (2)	20.06 (5)	18.93	20.24
GdHL	4.74 (1)	4.45 (2)	2.18	1.89
GdH_2L	2.07 (1)	2.11 (3)	–	–
LuL	22.06 (3)	21.65 (4)	21.22	21.85
LuHL	4.65 (2)	4.47 (4)	–	–

[a] Ref. [13]. [b] Ref. [19]. [c] Spectrophotometry, $[H^+] = 0.01$–1.0 M, $I = [H^+] + [Na^+] = 0.15$ M in samples at $[H^+] < 0.15$ M.

The stability constants of Ln(AAZTA-C_2-COO^-) and Ln(AAZTA-C_4-COO^-) complexes like the parent Ln(AAZTA) complexes increase from La^{3+} to Lu^{3+} (Table 2). These data clearly reflect the effect of the flexible coordination cage formed by the three nitrogen and four carboxylate oxygen atoms of the ligands, which results in an improved size match for the Ln^{3+} ions with the smaller ionic radius.

The Ca^{II}, Zn^{II}, and Ln^{III} complexes of AAZTA-C_2-COO^- and AAZTA-C_4-COO^-, similarly to the behavior shown by the analogous AAZTA complexes, can be protonated at low pH values. The logK_{MHL} values of Ca^{II}, Zn^{II}, Cu^{II}, and Ln^{III} complexes with AAZTA-C_2-COO^- and AAZTA-C_4-COO^- ligands (Table 2) are very similar to the logK_3^H value of the free ligands (Table 1). The experimental evidence clearly indicates that the propionic acid and the *n*-valeric acid side chains of AAZTA-C_2-COO^- and AAZTA-C_4-COO^- ligands do not participate in the coordination to metal ions, as this functionality can protonate/deprotonate independently. At lower pH values, one and two smaller protonation constants could be determined for the Zn^{II} and Cu^{II} complexes, which might be explained by the presence of one or two weakly coordinated donor atoms (a carboxylate oxygen), which can be protonated in the pH range of 2 to 4.

Relaxation properties of Gd(AAZTA-C_2-COO^-) and Gd(AAZTA-C_4-COO^-)

Relaxivity values (r_{1p}) of Gd(AAZTA), Gd(AAZTA-C_2-COO^-), and Gd(AAZTA-C_4-COO^-) as a function of pH are shown in Figure 1.

The relaxivity values of Gd(AAZTA-C_2-COO^-) and Gd(AAZTA-C_4-COO^-) are 8.8 $mM^{-1}s^{-1}$ and 9.4 $mM^{-1}s^{-1}$, respectively, at pH 7.4, 21 MHz, and 298 K. The pH dependence of relaxivity shown in Figure 1 has a similar behaviors for the two complexes. The r_{1p} values remain almost constant in the range of pH 2–11 whereas they significantly increase below pH 2 and decrease above pH 11 for both complexes. The high relaxivity values obtained in strong acidic conditions have to be associated with acidic hydrolysis suffered by the complexes. At low

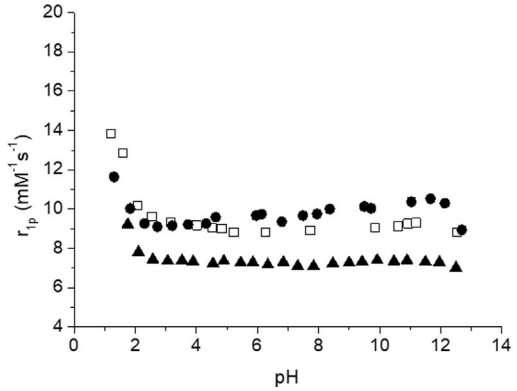

Figure 1. Relaxivity values (r_{1p}) of Gd(AAZTA) (π), Gd(AAZTA-C_2-COOH) (≤), and Gd(AAZTA-C_4-COOH) (●) as a function of pH ([GdL] = 1.0 mM, 21 MHz, 25 °C).

pH, these species are highly protonated with a consequent release of the paramagnetic Gd^{3+} ions, which are characterized by high relaxivity (12.98 $mM^{-1}s^{-1}$ at 21 MHz and 25 °C). From pH 11–12, hydrolysis of the coordinated water molecules may take place with a consequent decrease of the relaxivity values.

When comparing the relaxivity values of the herein investigated Gd^{III} complexes with those of previously reported $q = 2$ Gd^{III} complexes, it comes evident that they are higher than that expected from the plot of relaxivity as a function of molecular weight (Figure 2). This enhancement in relaxivity can, in principle, be ascribed to either a lengthened molecular reorientation owing to some kind of aggregation and/or a contribution from second-sphere water molecules.[24] The first hypothesis was checked by measuring the relaxation rate of Gd(AAZTA-C_2-COO^-) and Gd(AAZTA-C_4-COO^-) as a function of their concentration in the range 0.05–3.5 mM (see the Supporting Information, Figure S2), at neutral pH, 25 °C, and 21 MHz. A slight deviation from linearity is observed, for both Gd complexes, above concentrations of approximately 0.1 mM, indicating the likely occurrence of a concentration-dependent aggregation process. Linear fitting of data at a concentration of < 0.1 mM afforded relaxivity values of 7.7 and 8.6 $mM^{-1}s^{-1}$ for Gd(AAZTA-C_2-COO^-) and Gd(AAZTA-C_4-COO^-), respectively. These values still fall slightly above the line of expected values on the basis of molecular weight, leading to assumption of an additional contribution from second-sphere water molecules.

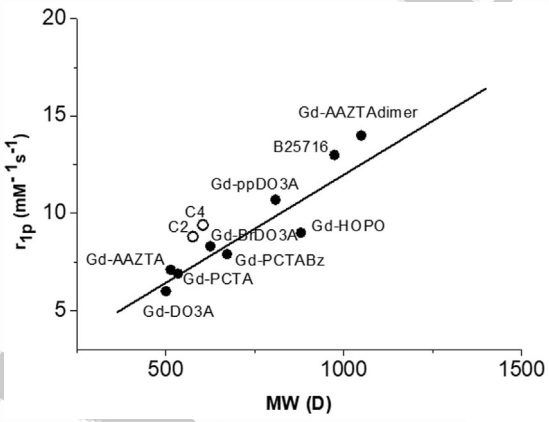

Figure 2. Molecular weight (M_W) dependence of the relaxivity (0.47 T, 298 K) for typical Gd^{III} complexes with two inner-sphere water molecules. See ref. [10] and references herein.

To determine the kinetic parameters governing the water exchange process, the transversal relaxation rate (R_{2p}) of the ^{17}O nucleus of $^{17}OH_2$ were determined by ^{17}O NMR spectroscopy at variable temperature (273–346 K)[25] in the presence of Gd(AAZTA-C_2-COO^-) and Gd(AAZTA-C_4-COO^-) complexes (Figure 3). Overall, all three investigated systems show similar transverse relaxivity values ($R_{2p} = R_{2(complex)} - R_{2(control)}$) and are consistent with the presence of two inner-sphere water molecules as for the parent Gd(AAZTA). However, whereas Gd(AAZTA) shows a single, pretty-defined bell-shaped profile, in the case of Gd(AAZTA-C_2-COO^-) and Gd(AAZTA-C_4-COO^-) derivatives, there is clear evidence of an additional species, which shows up in the low temperature measurements (273–283 K).

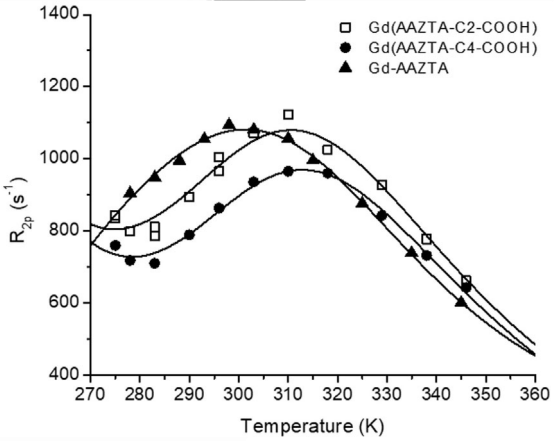

Figure 3. Comparison of the temperature dependence of the reduced transverse ^{17}O water relaxation (R_{2p}) for Gd(AAZTA-C_2-COO^-) (≤), Gd(AAZTA-C_4-COO^-) (●), and Gd(AAZTA) (π) at 14.09 T, pH 7.4 ([GdL] = 20.0 mM).

The profiles obtained for the two Gd(AAZTA) derivatives suggest that the inner-sphere water molecules in these species display both fast- and slow-regime exchange rates. The analysis of the observed profiles by using the modified Swift–Connick equations[26] yielded the following results: for Gd(AAZTA-C_2-COO^-), the water molecules in fast exchange with the bulk solvent molecules are characterized by a τ_M value of 7.0 ns and weight for about 35% of the total whereas 65% of water molecules are characterized by a τ_M value of 330 ns. In the case of Gd(AAZTA-C_4-COO^-), an analogous population distribution is observed with the corresponding values being 7.6 ns and 286 ns, respectively.

In principle, the presence of fast and slow exchanging populations might be ascribed either to the structurally different water molecules on the same molecule or to the presence of two distinct solution species endowed with different structures. The observation of a 35/65 distribution of the two kind of molecules between the slow and fast regime in the Gd(AAZTA-C_4-COO^-) derivative lends support to the hypothesis of the

presence of the isomeric species as frequently observed in the case of solutions of macrocyclic Ln^{III} complexes.[27]

To get more insight into the solution structures of the two *n*-alkyl acid derivatives of Gd(AAZTA), we acquired the high-resolution ^{1}H NMR spectra of the corresponding Eu^{III} and Yb^{III} complexes. Recently published variable-temperature (VT)-^{1}H NMR spectra of the Ln(AAZTA) complexes were also considered.[20] As shown in Figures S2–S6 (in the Supporting Information), the ^{1}H NMR spectra showed a pattern made of half the number of methylenic protons present in each of the considered AAZTA ligands. The observed pattern did not change over an extensive range of temperature (274–313 K), indicating the occurrence of a fast dynamic process that hampers the detection of "frozen" structures. Actually, by passing from water to a D_2O/[D_6]DMSO (60/30 vol%) mixture, it was possible to acquire spectra down to 248 K (Figures S2 and S5 in the Supporting Information). Inspection of the lowest temperature spectra allowed us to access differences in the broadening of the resonances, which may be suggestive of an incipient coalescence process. The observed behavior is taken as additional support for the hypothesis for the presence, in solution, of two interconverting isomers, differing for the exchange regime of the coordinated water molecules.

More information on the determinants of the observed relaxivity was obtained recording the $1/T_1$ NMRD profiles over an extended range of magnetic field strengths (0.01–80 MHz as proton Larmor frequency). The NMRD profiles measured at neutral pH, 25 °C and 37 °C for Gd(AAZTA-C_2-COO^-) and Gd(AAZTA-C_4-COO^-), are shown in Figure 4. Experimental data were fitted by using the SBM (Solomon–Bloembergen–Morgan) theory to extract the relaxometric parameters (Δ^2, τ_V, and τ_R) reported in Table 3. In the fitting procedure, the values of τ_M for the two derivatives were kept fixed to the weighted average of the values determined by ^{17}O NMR-R_{2p}.

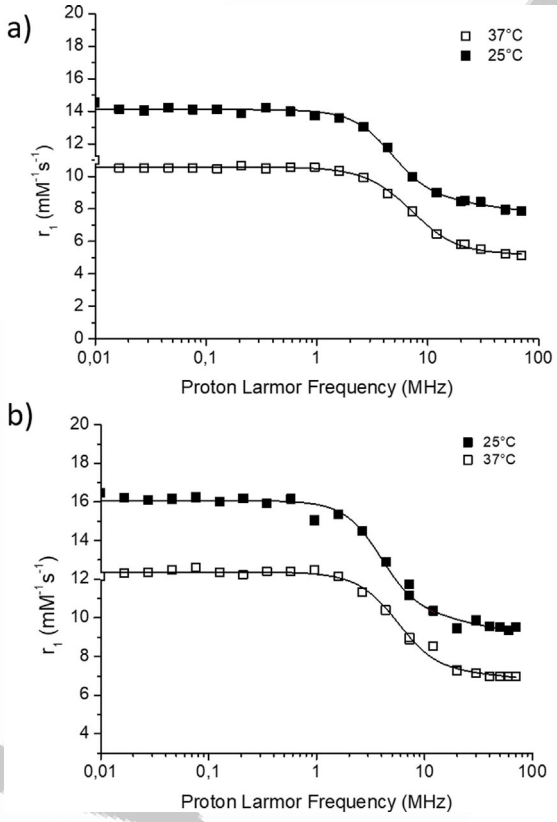

Figure 4. $1/T_1$ NMRD profile from 0.01 to 80 MHz of 1 mM aqueous solutions of Gd(AAZTA-C_2-COOH) (a) and Gd(AAZTA-C_4-COOH) (b) at pH 7 and 25 °C (') and 37 °C (○).

Table 3. Relaxation parameters of the Gd(AAZTA-C_2-COO^-), Gd(AAZTA-C_4-COO^-), and Gd(AAZTA) complexes as derived from fitting of $^{17}O R_{2p}$ versus temperature and NMRD profiles (25 °C).

		Gd(AAZTA-C_4-COOH)	Gd(AAZTA-C_2-COOH)	Gd(AAZTA)[g]
r_{1p} (0.47 T, 298 K)		9.4	8.8	7.1
$\Delta^2 \times 10^{19}$ [s^{-2}][a]		2.3 ± 0.21	3.2 ± 0.24	2.15
τ_V [ps][b]		32.6 ± 2.9	26.1 ± 1.7	31.0
τ_R [ps][c]		115 ± 2.2	92 ± 1.5	74
τ_M [ns][d]	species 1	7.6 (35%)	7.0 (35%)	90
	species 2	286 (65%)	331 (65%)	
q[e]		2	2	2
q_{SS}[f]		1	1	0

[a] Squared mean transient zero-field splitting (ZFS) energy as obtained from fitting of NMRD profiles. [b] Correlation time for the collision-related modulation of the ZFS Hamiltonian as obtained from fitting of NMRD profiles. [c] Re-orientational correlation time as obtained from fitting of NMRD profiles. [d] Exchange life-time of the coordinated water molecules as obtained from fitting of $^{17}O R_{2p}$ vs. *T* profiles of Figure 3. [e] Number of inner-sphere water molecules as obtained from fitting of NMRD profiles. [f] Number of second-sphere water molecules as obtained from fitting of NMRD profiles. [g] Ref. [17].

The best fitting of experimental data afforded the presence of one second-sphere water molecule for both Gd(AAZTA-C_2-COO^-) and Gd(AAZTA-C_4-COO^-), which was not present in the parent Gd(AAZTA). This result supported the suggestion related to the observation that the proton relaxivity values at 21.5 MHz (Figure 2) fall slightly above the line of expected values calculated on the basis of the molecular weights. This additional contribution from second-sphere water molecules is likely related to the presence on the herein reported complexes of the acidic alkyl function, which is expected to enhance the overall hydrophilic character of the complexes.

Transmetallation of Gd(AAZTA-C_2-COO^-) and Gd(AAZTA-C_4-COO^-) complexes with Cu^{2+}

Besides the high thermodynamic stability, GBCAs must be characterized by high kinetic inertness to avoid the in vivo dissociation of the Gd^{III} complexes. Actually, it has been realized that the kinetic inertness is more important than the absolute value of the stability constant for in vivo applications of Gd^{III} complexes.[3,28–30] Body fluids are very complex systems and the in vivo study of the rate of dissociation reactions of Gd^{III} complexes is considered a difficult task.[31–33] However, in vitro studies are usually quite suitable to predict the kinetic behav-

ior of the Gd^{III} complexes under in vivo conditions. The kinetic inertness of Gd(AAZTA) was assessed by investigating the rates of the transmetallation reaction with the use of Cu^{2+} or Eu^{3+} as exchanging ions.[18] For a direct comparison of the kinetic properties of Gd(AAZTA-C_2-COO^-), Gd(AAZTA-C_4-COO^-), and Gd(AAZTA), the same method and identical conditions were used as previously used for Gd(AAZTA).[18] The rates of the transmetallation reactions were studied by spectrophotometry in the presence of Cu^{2+} as exchanging metal ion. Mechanism proposed for the transmetallation reactions of the Gd(AAZTA-C_2-COO^-) and Gd(AAZTA-C_4-COO^-) with Cu^{2+} are summarized in Scheme 4. Experimental details and equations used to evaluate the kinetic parameters are summarized in the Supporting Information. The rate and equilibrium constants that characterize the transmetalation reaction of Gd(AAZTA-C_2-COO^-) and Gd(AAZTA-C_4-COO^-) are shown and compared with those of Gd(AAZTA) in Table 4. In our experimental conditions (pH 2.8–5.0), the dominating species is Gd(HL) with the protonated *n*-propionate and *n*-valerate pendants.

According to the proposed mechanism, the dissociation of the Gd(AAZTA) derivatives might take place by the proton- and metal-assisted pathways.[18] The proton-assisted dissociation of the Gd^{III} complexes generally takes place by the protonation of the complexes via the formation of protonated intermediates. The protonation of the Gd(AAZTA) derivatives presumably occurs on the carboxylate groups. The dissociation that might take place via proton transfer from the carboxylate group to the nitrogen atom, results in the displacement of the Gd^{3+} ion from the coordination cage and the release of the Gd^{3+}. The $k_{Gd(HL)}$ rate constants characterizing the dissociation rate of the monoprotonated Gd(AAZTA-C_2-COOH) and Gd(AAZTA-C_4-COOH) species are about 44 and 1500 times smaller than that of monoprotonated Gd(HAAZTA). As the protonation of the Gd(AAZTA-C_2-COO^-) and Gd(AAZTA-C_4-COO^-) takes place on the distant *n*-propionate and the *n*-valerate side chains, the proton transfer to the nitrogen atom is less probable than that of the Gd(HAAZTA) species with the protonated carboxylate group of the AAZTA skeleton. On the other hand, the dissociation rate of the double protonated Gd(HAAZTA-C_2-COOH) and Gd(HAAZTA-C_4-COOH) species ($k_{Gd(H2L)}$) are comparable with the $k_{Gd(HL)}$ value of the Gd(HAAZTA) species. As the second protonation of Gd(AAZTA-C_2-COO^-) and Gd(AAZTA-C_4-COO^-) and the first protonation of Gd(AAZTA) occur on the carboxylate group of the AAZTA unit, the dissociation of these protonated Gd^{III} complexes might take place with the similar probability. However, the somewhat lower $k_{Gd(H2L)}$ values of Gd(HAAZTA-C_2-COOH) and Gd(HAAZTA-C_4-COOH) than that of $k_{Gd(HL)}$ of Gd(HAAZTA) may be explained by the interaction between the Gd^{3+} ion and the basic nitrogen atoms of AAZTA-C_2-COO^- and AAZTA-C_4-COO^-. The stability constants of the hetero-dinuclear Gd(AAZTA-C_2-COO^-)Cu intermediate ($K_{Gd(L)Cu}$) is about 16 times higher than that of Gd(AAZTA)Cu, which can be explained by the coordination of the Cu^{II} ion by the more basic *n*-propionate side chain in the Gd(AAZTA-C_2-COO^-)Cu intermediate. The $k_{Gd(L)Cu}$ rate constant, characterizing the dissociation of the dinuclear Gd(AAZTA-C_2-COO^-)Cu intermediate is about two times smaller than that of Gd(AAZTA)Cu. Because of the stronger interaction, the functional groups of the AAZTA-C_2-COO^- ligand are transferred with the much smaller rate from the Gd^{III} to the attacking Cu^{II} ion with respect to what was found in the case of Gd(AAZTA). This hypothesis is further supported by the lack of the Cu^{2+}-assisted dissociation of the Gd(AAZTA-C_4-COO^-) complex owing to the stronger coordination of the Gd^{3+} ion with the more basic nitrogen atoms of the ligand. Somewhat larger kinetic inertness of the Gd(AAZTA-C_4-COO^-) and Gd(AAZTA-C_2-COO^-) complexes is also confirmed by the calculated dissociation rate (k_d) and half-life ($t_{1/2}$) values at pH 7.4. The k_d and $t_{1/2}$ values in Table 4 reveal that the dissociation of Gd(AAZTA-C_2-COO^-) and Gd(AAZTA-C_4-COO^-) complexes is slightly slower than that of Gd(AAZTA).

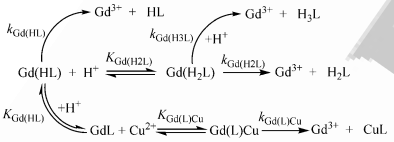

Scheme 4. Proposed mechanism of the transmetallation reactions for the Gd(AAZTA-C_2-COO^-) and Gd(AAZTA-C_4-COO^-) complexes. The lower and the last upper paths are valid for the Gd(AAZTA-C_2-COO^-) and Gd(AAZTA-C_4-COO^-) complexes, respectively.

Table 4. Rate (k_i) and equilibrium constants (K_i) and half-lives ($t_{1/2} = \ln 2/k_d$) for the transmetallation reactions of Gd(AAZTA-C_4-COO^-), Gd(AAZTA-C_2-COO^-), and Gd(AAZTA) complexes (25 °C).

I	Gd(AAZTA-C_4-COO^-) 0.15 M NaCl	Gd(AAZTA-C_2-COO^-)	Gd(AAZTA)[a] 0.1 M KCl[b]
k_{GdHL} [s^{-1}]	$(7\pm2)\times10^{-6}$	$(2\pm2)\times10^{-5}$	4.5×10^{-3}
$k_{Gd(H2L)}$ [s^{-1}]	$(2.3\pm0.2)\times10^{-3}$	$(2.2\pm0.1)\times10^{-3}$	–
$k_{Gd(H3L)}$ [s^{-1}]	1.2 ± 0.3	–	–
$k_{Gd(L)Cu}$ [s^{-1}]	–	$(1.0\pm0.1)\times10^{-5}$	2.1×10^{-5}
$K_{Gd(HL)}$ [M^{-1}]	54 954 (pH-pot.)	28 183 (pH-pot.)	233
$K_{Gd(H2L)}$ [M^{-1}]	118 (pH-pot.)	128 (pH-pot.)	–
$K_{Gd(L)Cu}$ [M^{-1}]	–	166 ± 40	9
k_d [s^{-1}], pH 7.4	1.4×10^{-8}	2.3×10^{-8}	4.0×10^{-8}
$t_{1/2}$ [h], pH 7.4	1.3×10^{4}	1.0×10^{4}	4.3×10^{3}

[a] Ref. [18].

Conclusion

Two functionalized Gd(AAZTA) derivatives have been successfully synthetized and characterized. They appear promising systems for further conjugation to substrates of interest. Moreover, it was found that they show improved relaxation properties and slightly better thermodynamic and kinetic behavior when compared with those of the parent Gd(AAZTA). Therefore, the body of these results leads us to conclude that these complexes are good candidates as contrast agents for further MRI applications either on their own or as systems for the design of targeting agents. Relaxometric studies demonstrated that these complexes presented improved relaxivity values ($r_{1p} = 8.8$ mM^{-1}s^{-1} and 9.4 mM^{-1}s^{-1} for the derivatives with C_2 and C_4 spacers, respectively, in comparison to Gd(AAZTA) ($r_{1p} =$

7.1 $mM^{-1}s^{-1}$). ^{17}O and ^{1}H NMR spectra results suggest the presence in solution of species containing water molecules in two distinct motion regimes. The observation of fast and slow water exchanging isomers is not uncommon in lanthanide(III) macrocyclic complexes and it is usually accompanied by the observation of the corresponding sets of signals in the corresponding ^{1}H NMR spectra of the analogs with other Ln^{III} ions. Herein, the interconversion appears too fast to be slowed down in the high-resolution NMR spectra.

A corollary to these observations is that, for the first time to our knowledge, it has been possible, in the field of Ln^{III}-containing complexes, to extract fundamental information on the presence of two interconverting isomers from the ^{17}O NMR data when the high-resolution NMR spectra were completely non-informative.

Experimental Section

General

All standard chemicals were acquired from Merck and VWR. The new compounds were characterized by using ^{1}H and ^{13}C NMR spectroscopy. ^{1}H and ^{13}C NMR spectra were recorded at 298 K with a Bruker spectrometer (600 MHz for ^{1}H). UPLC (ultra-performance liquid chromatography) analytical characterizations were carried out by using a Waters UPLC-H-Class system equipped with Acquity QDa MS detector and dual-wavelength UV/Vis TUV detector. Purification by using HPLC was performed with a system equipped with a Waters 2767 autosampler and autoinjector, Waters 2525 pumps, Waters 3100 MS Detector, and Waters 2998 photodiode array (PDA) detector, with an Atlantis dC18 OBD Prep Column, 100 Å, 5 μm, 19 mm × 100 mm. Water with 0.1% TFA (A) and acetonitrile with 0.1% TFA (B) were used as eluents.

Synthesis of H_4AAZTA-C_4-COOH ligand (Scheme 2)

Compound 1

N,N′-Dibenzylethylenediamine (28.6 mmol, 6.7 mL) was suspended in EtOH (50 mL) and the mixture was stirred until a clear solution was obtained. Paraformaldehyde (86 mmol, 2.6 g) was added and the suspension was stirred and heated at 80 °C for 1.5 h. The solution of 6-nitrohexanoic acid methyl ester (28.6 mmol, 5 g) in EtOH (10 mL) was added dropwise. The new solution was left to cool to room temperature and stirred for 18 h. The mixture was evaporated and the residue dissolved in ethyl acetate (EtOAc) was purified by flash chromatography (silica gel column, 90:10 petroleum ether/EtOAc) to give **1** as a pale-yellow oil (7.4 g, 60%). ^{1}H NMR ($CDCl_3$): $\delta = 7.32$ (m, 10H), 3.76 (d, 2H, $J = 13$ Hz), 3.67 (s, 3H), 3.60 (d, 2H, $J = 13$ Hz), 3.53 (d, 2H, $J = 14.2$ Hz), 2.98 (d, 2H, $J = 14.2$ Hz), 2.64 (m, 4H), 2.13 (t, 2H, $J = 7.5$ Hz), 1.59 (m, 2H), 1.32 (m, 2H), 0.79 ppm (m, 2H); ^{13}C NMR (CDCl3): $\delta = 173.1$, 138.5, 128.5, 127.6, 126.5, 94.1, 63.4, 60.8, 58.1, 50.9, 36.0, 32.9, 23.9, 21.9 ppm; ESI-MS (*m/z*): $[M+H]^+$ 440.5 (obsd.), 440.5 (calcd for $C_{25}H_{34}N_3O_4$).

Compound 3

Palladium on carbon (1.0 g) was slowly added to a solution of compound **1** (15.5 mmol; 6.8 g) in MeOH (300 mL). The suspension was stirred at 40 °C for 5 h under hydrogen atmosphere. The suspension was filtered through a bed of Celite and concentrated in vacuo. The residue was dissolved in acetonitrile (MeCN; 75 mL) and then freshly ground K_2CO_3 (80.2 mmol; 11.0 g) and Na_2SO_4 (15.0 mmol; 2.1 g) were added. *tert*-Butyl bromoacetate (71.0 mmol; 10.4 g) was added and the orange mixture was stirred and heated at 80 °C for 20 h. The mixture was filtered, evaporated, and the residue was purified by chromatography (silica gel column, 30:5 *n*-hexane/EtOAc to give a pale-yellow oil (6.0 g; 57%). ^{1}H NMR ($CDCl_3$): $\delta = 3.66$ (s, 3H; OCH_3), 3.61 (s, 4H), 2.69–3.01 (br, 6H), 2.32 (t, 2H, $J = 7.5$ Hz), 1.53–1.64 (br, 6H), 1.45 ppm (s, 36H); ^{13}C NMR ($CDCl_3$): $\delta = 173.3$, 172.0, 81.3, 80.4, 65.5, 62.8, 61.5, 60.6, 51.2, 50.8, 35.8, 33.2, 27.5, 24.8, 21.5 ppm; ESI-MS (*m/z*): $[M+H]^+$ 686.6 (obsd.), 686.5 (calcd for $C_{35}H_{64}N_3O_{10}$).

Compound 4

A 1 M solution of LiOH (23.0 mmol; 23.0 mL) was added dropwise to a solution of compound **3** (2.9 mmol; 2.0 g) in tetrahydrofuran (THF; 50 mL) cooled at 0 °C. The solution was then stirred at room temperature for 28 h. The pH was brought to 7.0 by addition of HCl 6 M. Water (45 mL) was added and THF was evaporated. The aqueous residue was extracted with EtOAc (3 × 75 mL). The organic phases were collected, dried with Na_2SO_4, filtered, and concentrated in vacuo. The crude was purified by chromatography (silica gel column, 3:2 *n*-hexane/EtOAc) to give **4** as a pale-yellow oil (1.0 g; 54%). ^{1}H NMR ($CDCl_3$): $\delta = 3.63$ (s, 4H), 3.16 (br, 6H), 2.41 (t, 2H, $J =$ ■■ Hz), 1.61–1.67 (br, 6H), 1.48 ppm (s, 36H); ^{13}C NMR ($CDCl_3$): $\delta = 178.7$, 173.2, 171.0, 81.6, 80.7, 65.3, 63.3, 61.5, 60.3, 37.4, 34.3, 29.0, 27.5, 21.4 ppm; ESI-MS (*m/z*): $[M+H]^+$ 672.6 (obsd.), 672.4 (calcd for $C_{34}H_{62}N_3O_{10}$); $[M+Na]^+$ 694.6 (obsd.), 694.8 (calcd).

Compound 5 (H_4AAZTA-C_4-COOH)

Trifluoroacetic acid (20 mL) was added dropwise to a solution of **4** (1.0 g, 1.50 mmol) and triisopropylsilane (0.6 mL) in CH_2Cl_2 (5 mL) cooled to 0–5 °C. The solution was stirred at room temperature for 20 h, then evaporated. The residue dissolved in H_2O (5 mL) was purified by HPLC under isocratic conditions (98:2, A/B) at a flow rate of 20 mL min^{-1}. The pure product was obtained as a white powder (0.40 g, yield 60%) and characterized by UPLC-UV-MS-ESI(+) by using an Acquity UPLC HSS T3 column, 100 Å, 1.8 μm, 2.1 mm × 100 mm and 0.05% TFA in water (A) and 0.05% TFA in acetonitrile (B) as solvents. Elution: initial conditions 0% B, isocratic 0% B over 0.56 min, gradient 0–10% B over 2.5 min, 10–30% B over 6 min, 30–100% B over 10 min, flow rate 0.4 mL min^{-1} and UV detection at 220 nm (t_R, retention time = 3.9 min, purity 95.0%). ^{1}H NMR (D_2O): $\delta = 3.80$ (d, 4H, $J = 5.1$ Hz), 3.71 (s, 4H), 3.60 (m, 2H), 3.44 (s, 6H), 2.31 (t, 2H, $J = 7.2$), 1.50 (m, 2H), 1.26 ppm (m, 2H); ^{13}C NMR (D_2O): $\delta = 177.8$, 175.6, 169.8, 61.9, 59.3, 57.8, 51.8, 51.5, 33.2, 32.6, 23.8, 21.4 ppm; ESI-MS (*m/z*): $[M+H]^+$ 448.3 (obsd.), 448.4 (calcd for $C_{18}H_{30}N_3O_{10}$).

Synthesis of H_4AAZTA-C_2-COOH (Scheme 3)

Compound 1a

N,N′-Dibenzylethylenediamine (22.0 mmol, 5.3 mL) was suspended in EtOH (50 mL) and the mixture was stirred until a clear solution was obtained. Paraformaldehyde (66.0 mmol; 2.0 g) was added and the suspension was stirred and heated at 80 °C for 1.5 h. The solution of 2-nitroethanol (22.0 mmol; 2 g) in EtOH (10 mL) was added dropwise. The new solution was left to cool to room temperature and stirred for 18 h. The mixture was evaporated and the residue dissolved in ethyl acetate (EtOAc) was purified by flash chromatography (silica gel column, 80:20 petroleum ether/EtOAc) to give **1** as a pale-yellow oil (7.0 g, 90%). ^{1}H NMR ($CDCl_3$): $\delta = 7.33$ (m, 10H),

3.74 (d, 2H, $J=13$ Hz), 3.70 (s, 2H), 3.65 (d, 2H, $J=13$ Hz), 3.53 (d, 2H, $J=14.4$ Hz), 3.05 (d, 2H, $J=14.3$ Hz), 2.70 (m, 2H), 2.63 ppm (m, 2H); ^{13}C NMR ($CDCl_3$): $\delta=138.0$, 128.3, 127.7, 126.7, 94.0, 65.0, 63.1, 58.37, 58.0 ppm; ESI-MS (*m/z*): $[M+H]^+$ 356.2 (obsd.), 356.2 (calcd for $C_{20}H_{26}N_3O_3$).

Compound 2a

Compound **1a** (18.0 mmol; 6.3 g) was dissolved in dry THF (40 mL), *tert*-butyl acrylate (5.3 mL; 36.0 mmol) was added and the mixture was stirred at room temperature for 5 min. *t*BuOK (2.4 g; 21.6 mmol) was added to the solution, and stirring was continued at room temperature for 3 h. After removal of the solvent under reduced pressure, the residue was taken up in methanol and purified by chromatography (silica gel column, 90:10 petroleum ether/EtOAc) to give **2a** as a pale-yellow oil (3.9 g, 48%). ^{1}H NMR ($CDCl_3$): $\delta=7.31$ (m, 10H), 3.76 (d, 2H, $J=12.5$ Hz), 3.61 (d, 2H, $J=12.7$ Hz), 3.50 (d, 2H, $J=14$ Hz), 2.98 (d, 2H, $J=14$ Hz), 2.61 (m, 4H), 1.96 (m, 2H), 1.74 (m, 2H), 1.43 ppm (s, 9H); ^{13}C NMR ($CDCl_3$): $\delta=170.3$, 138.3, 128.3, 127.6, 126.6, 93.4, 80.0, 63.2, 61.0, 57.9, 31.0, 28.4, 27.3 ppm; ESI-MS (*m/z*): $[M+H]^+$ 454.3 (obsd.), 454.3 (calcd for $C_{26}H_{36}N_3O_4$).

Compound 3a

Palladium on carbon (0.3 g) was slowly added to a solution of compound **2a** (1.3 g; 2.8 mmol) in MeOH (50 mL). The suspension was stirred at 40 °C for 5 h under hydrogen atmosphere. The suspension was filtered through a bed of Celite and concentrated in vacuo. The residue was dissolved in acetonitrile (MeCN; 50 mL) and then freshly ground K_2CO_3 (2.0 g; 15 mmol) and Na_2SO_4 (0.36 g; 2.6 mmol) were added. Methyl bromoacetate (1.24 mL; 13.2 mmol) was added and the mixture was stirred and heated at 80 °C for 20 h. The mixture was filtered, more K_2CO_3 (2.0 g; 15 mmol), Na_2SO_4 (0.36 g; 2.6 mmol), and methyl bromoacetate (0.62 mL; 6.6 mmol) were added and the new mixture heated at 80 °C for 12 h. The mixture was filtered, evaporated, and the residue was purified by chromatography (silica gel column, 30:5 *n*-hexane/EtOAc to give a pale-yellow oil (0.7 g; 47%). ^{1}H NMR ($CDCl_3$): $\delta=3.75$ (s, 4H), 3.69 (s, 6H), 3.67 (s, 6H), 3.36 (s, 4H), 3.01 (d, 2H, $J=14.3$ Hz), 2.8 (m, 2H), 2.69 (m, 4H), 2.35 (m, 2H), 1.84 (m, 2H), 1.43 ppm (s, 9H); ^{13}C NMR ($CDCl_3$): $\delta=172.9$, 172.6, 171.0, 79.3, 63.6, 62.1, 60.4, 58.3, 50.8, 50.6, 31.3, 28.0, 27.4 ppm; ESI-MS (*m/z*): $[M+H]^+$ 532.2 (obsd.), 532.3 (calcd for $C_{24}H_{42}N_3O_{10}$).

Compound 4a

Trifluoroacetic acid (2 mL) was added dropwise to a solution of **3a** (0.5 g; 0.94 mmol) and triisopropylsilane (0.050 mL) in CH_2Cl_2 (2 mL) cooled to 0–5 °C. The solution was stirred at room temperature for 1 h. The mixture was co-evaporated with CH_2Cl_2 (3× 10 mL) and taken into the next step without further purification. ^{1}H NMR ($CDCl_3$): $\delta=3.89$ (s, 2H), 3.83 (s, 2H), 3.79 (s, 6H), 3.75 (s, 6H), 3.71 (s, 4H), 3.47–3.31 (m, 6H), 3.16 (d, 2H, $J=14.5$ Hz), 2.42 (t, 2H, $J=7.4$ Hz), 1.79 ppm (t, 2H, $J=7.4$ Hz); ^{13}C NMR ($CDCl_3$): $\delta=$ 175.4, 173.8, 167.3, 61.4, 60.0, 57.4, 52.9, 51.9, 51.8, 49.9, 29.2, 27.2 ppm; ESI-MS (*m/z*): $[M+H]^+$ 476.4 (obsd.), 476.2 (calcd for $C_{20}H_{34}N_3O_{10}$).

Compound 5a (H_4AAZTA-C_2-COOH)

A 1 M solution of LiOH (20.0 mmol; 20.0 mL) was added dropwise to a solution of compound **3a** (0.6 mmol; 0.4 g) in tetrahydrofuran (THF; 40 mL) cooled at 0 °C. The solution was then stirred at room temperature for 28 h. The pH was adjusted to 7.0 by addition of HCl 6 M. Water (45 mL) was added and THF was evaporated. The aqueous residue was purified by HPLC under isocratic conditions (98:2, A/B) at a flow rate of 20 mL min^{-1}. The pure product was obtained as a white powder (0.10 g, yield 39%) and characterized by UPLC-UV-MS-ESI(+) by using the method described for compound **5** ($t_R=2.5$ min, purity 92.0%). ^{1}H NMR (D_2O): $\delta=3.80$ (s, 4H), 3.71 (s, 4H), 3.40 (m, 2H), 3.32 (s, 6H), 2.38 (t, 2H, $J=8.0$ Hz), 1.68 ppm (t, 2H, $J=8.0$ Hz); ^{13}C NMR (D_2O): $\delta=176.3$, 176.1, 170.4, 61.3, 59.2, 57.7, 52.2, 50.2, 28.5, 27.1 ppm; ESI-MS (*m/z*): $[M+H]^+$ 420.2 (obsd.), 420.1 (calcd for $C_{16}H_{26}N_3O_{10}$).

Synthesis of Ln^{III} complexes

Aqueous solutions of $GdCl_3$ or $EuCl_3$ and ligands were mixed at 1:1 concentration ratio ($[GdCl_3]=[EuCl_3]=[H_4AAZTA\text{-}C_4\text{-}COOH]=[H_4AAZTA\text{-}C_2\text{-}COOH]=50$ mM). The solutions were stirred for 4 h. The pH of the solutions was maintained at 7 by the addition of solid NaOH. The occurrence of residual free Ln^{3+} ion was assessed by UV/Vis spectroscopy by using the xylenol orange test.[34] The amount of the residual free Ln^{3+} ion was less than 0.3% (mol mol^{-1}). The Ln^{III} complexes were characterized by the direct-infusion method using ESI-MS (Waters 3100) in negative ion mode Gd(AAZTA-C_2-COOH): ESI- MS (−): *m/z*: calculated for $C_{16}H_{21}GdN_3O_{10}$ $[M-H]^-$: 573.0, found: 573.1; Eu(AAZTA-C_2-COOH): ESI- MS (−): *m/z*: calculated for $C_{16}H_{21}EuN_3O_{10}$ $[M-H]^-$: 568.0, found: 568.1; Gd(AAZTA-C_4-COOH): ESI- MS (−): *m/z*: calculated for $C_{18}H_{25}GdN_3O_{10}$ $[M-H]^-$: 601.0, found: 601.2; Eu(AAZTA-C_4-COOH): ESI-MS (−): *m/z*: calculated for $C_{18}H_{25}EuN_3O_{10}$ $[M-H]^-$: 596.0, found: 596.2. The concentration of the Gd^{III} complexes was determined by ^{1}H NMR relaxometry after remineralization for 24 h at 120 °C in concentrated HCl solution (37%, v/v).

Thermodynamic studies

Materials

The chemicals used for the experiments were of the highest analytical grade. The concentration of the $CaCl_2$, $ZnCl_2$, $CuCl_2$, and $GdCl_3$ solutions were determined by complexometric titration with standardized Na_2H_2EDTA and xylenol orange ($ZnCl_2$, and $LnCl_3$), murexid ($CuCl_2$), and Patton & Reeder ($CaCl_2$) as indicators. The concentration of the H_4AAZTA, $H_4AAZTA\text{-}C_2\text{-}COOH$, and $H_4AAZTA\text{-}C_4\text{-}COOH$ was determined by pH-potentiometric titration in the presence and absence of a large (40-fold) excess of $CaCl_2$. The pH-potentiometric titrations were made with standardized 0.2 M NaOH.

Equilibrium measurements

The stability and protonation constants of Ca^{II}, Zn^{II}, and Ln^{III} complexes formed with AAZTA-C_2-COO^- and AAZTA-C_4-COO^- ligands were determined by pH-potentiometric titration. The metal-to-ligand concentration ratio was 1:1 (the concentration of the ligand was generally 0.002 M). In calculating the equilibrium constants of the metal complexes, the best fitting of the NaOH–pH data pairs, were obtained by assuming the formation of ML, MHL, MH_2L, MH_3L, MH_4L, and MLH_{-1} complexes in the 1.7–12.0 pH range. For the pH measurements and titrations, a Metrohm 888 Titrando titration workstation Metrohm-6.0234.110 combined electrode was used. Equilibrium measurements were carried out at a constant ionic strength (0.15 M NaCl) in 6 mL samples at 25 °C. The solutions were stirred, and N_2 was bubbled through them. The titrations were made in the pH range of 1.7–12.0. KH-phthalate (pH 4.005) and borax (pH 9.177) buffers were used to calibrate the pH meter.

For the calculation of $[H^+]$ from the measured pH values, the method proposed by Irving et al. was used as follows.[35] A 0.01 M HCl solution was titrated with standardized NaOH solution at 0.15 M NaCl ionic strength. The differences (A) between the measured (pH_{read}) and calculated pH ($-\log[H^+]$) values were used to obtain the equilibrium H^+ concentration from the pH values measured in the titration experiments ($A = 0.024$). For the equilibrium calculations, the stoichiometric water ionic product (pK_w) was also needed to calculate $[OH^-]$ values under basic conditions. The V_{NaOH}–pH_{read} data pairs of the HCl–NaOH titration obtained in the pH range 10.5–12.0 were used to calculate the pK_w value ($pK_w = 13.85$).

The stability constants of the $Cu(AAZTA)^{2-}$, $Cu(AAZTA\text{-}C_2\text{-}COO^-)^{3-}$, and $Cu(AAZTA\text{-}C_4\text{-}COO^-)^{3-}$ complexes were determined by a spectrophotometry study of the competition reaction between the Cu^{2+} and H^+ for the AAZTA, AAZTA-C_2-COO^-, and AAZTA-C_4-COO^- at the absorption band of $Cu(AAZTA)^{2-}$, $Cu(AAZTA\text{-}C_2\text{-}COO^-)^{3-}$, and $Cu(AAZTA\text{-}C_4\text{-}COO^-)^{3-}$ in the wavelength range 400–800 nm. The concentration of Cu^{2+}, AAZTA, AAZTA-C_2-COO^-, and AAZTA-C_4-COO^- was 0.002 M, whereas that of the H^+ was varied between 0.01 and 1.0 M (six samples). The H^+ concentration in the samples was adjusted with the addition of the calculated amounts of 3 M HCl. The ionic strength of the samples was adjusted to 0.15 M ($[H^+] \leq 0.15$ M $\rightarrow [Na^+] + [H^+] = 0.15$ M). The samples were kept at 25 °C for 7 days to attain the equilibrium (the time needed to reach the equilibria was determined by spectrophotometry). The absorbance values of the samples were determined at 11 wavelengths (575, 595, 615, 635, 655, 675, 695, 715, 735, 755, and 775 nm). For the equilibrium calculations, the protonation constants of the $Cu(AAZTA)^{2-}$, $Cu(AAZTA\text{-}C_2\text{-}COO^-)^{3-}$, $Cu(AAZTA\text{-}C_4\text{-}COO^-)^{3-}$ and the molar absorptivities of the Cu^{2+}, CuL, Cu(HL), $Cu(H_2L)$, $Cu(H_3L)$, and $Cu(H_4L)$ species were used. The protonation constants of the complexes $Cu(AAZTA)^{2-}$, $Cu(AAZTA\text{-}C_2\text{-}COO)^{3-}$, and Cu(AAZTA-C4-COO)$^{3-}$ were determined by pH-potentiometric titrations, made at 1:1 metal-to-ligand concentration ratios. The molar absorptivities of the Cu^{2+}, CuL, Cu(HL), $Cu(H_2L)$, $Cu(H_3L)$, and $Cu(H_4L)$ species were determined at 11 wavelengths (575, 595, 615, 635, 655, 675, 695, 715, 735, 755, and 775 nm) by recording the spectra of 1, 2, and 3 mM $Cu(AAZTA)^{2-}$, $Cu(AAZTA\text{-}C_2\text{-}COO^-)^{3-}$, and $Cu(AAZTA\text{-}C_4\text{-}COO^-)^{3-}$ solutions in the pH range 1.7–6.0 (0.15 M NaCl, 25 °C). The pH was adjusted by stepwise addition of concentrated NaOH or HCl. The spectrophotometric measurements were made with the use of a PerkinElmer Lambda 365 UV/Vis spectrophotometer at 25 °C, using 1.0 cm cells. The protonation and stability constants were calculated with the PSEQUAD program.[36]

Kinetic studies of the transmetallation reactions

The kinetic inertness of the $Gd(AAZTA\text{-}C_2\text{-}COO^-)^{2-}$ and $Gd(AAZTA\text{-}C_4\text{-}COO^-)^{2-}$ complexes was characterized by the rates of the exchange reactions taking place between the GdL and Cu^{2+}. The transmetallation reactions with Cu^{2+} were studied by spectrophotometry, by following the formation of the Cu^{II} complexes at 300 nm with a PerkinElmer Lambda 365 UV/Vis spectrophotometer. The concentration of the GdL complexes was 1×10^{-3} M, whereas the concentration of the Cu^{2+} was 20, 30, 40, or 50 times larger, to guarantee pseudo-first-order conditions. The temperature was maintained at 25 °C and the ionic strength of the solutions was kept constant, 0.15 M for NaCl. The exchange rates were studied in the pH range of about 2.8–5.0. To keep the pH values constant, monochloroacetic acid (pH range 2.8–3.1), *N*,*N*′-dimethylpiperazine (pH range 3.1–4.1), and *N*-methylpiperazine (pH range 4.1–5.2) buffers (0.01 M) were used. The pseudo-first-order rate constants (k_d) were calculated by fitting the absorbance data to Equation (5)

$$A_t = (A_0 - A_p)e^{-k_d t} + A_p \quad (5)$$

where A_t, A_0, and A_p are the absorbance values at time t, the start of the reaction, and at equilibrium, respectively.

Relaxometric studies

The observed longitudinal water protons relaxation rates (R_{1obs}) were measured by using a Stelar Spinmaster (Mede, Pavia, Italy) spectrometer operating at 0.47 T and employing a standard inversion-recovery (IR) pulse sequence (16 experiments, 2 scans). A typical 90° pulse width was 3.5 μs and the reproducibility for the longitudinal relaxation times (T_1) were ±0.5%. NMRD profiles were obtained by using a Stelar SpinMaster FFC-NMR relaxometer from 0.01–20 MHz and a Bruker WP80 NMR electromagnet for variable higher-field measurements (21.5–80 MHz), both equipped with a Stelar VTC-91 air-flow heater equipped with copper/constant thermocouple (uncertainty ±0.1 °C) for temperature control.

NMR studies

The VT-^{1}H NMR spectra of Eu^{III} and Yb^{III} complexes were recorded with Bruker Avance III (9.4 T) and Avance 600 (14.09 T) spectrometers, equipped with 5 mm probes and using a D_2O solution as internal lock. The temperature was controlled with Bruker thermostating units, and high-resolution spectra have been acquired by varying the temperature from 278 K to 350 K. Variable-temperature ^{17}O NMR measurements were performed with a Bruker Avance spectrometer, equipped with a 5 mm probe and using a capillary containing D_2O as external lock. The experimental settings were: spectral width 1000 Hz, 90° pulse (7 μs), acquisition time 10 ms, 1000 scans, and no sample spinning. Aqueous solutions containing 2.6% of the ^{17}O isotope (Yeda, Israel) were used. The observed transverse relaxation rates (R_2) were calculated from the signal width at half-height ($\Delta\nu_{1/2}$): $R_2^{obs} = \pi \times \Delta\nu_{1/2}$. Paramagnetic contributions to the observed transversal relaxation rate (R_{2p}) were calculated by subtracting from R_2^{obs} the diamagnetic contribution measured at each temperature value on pure water enriched with 2.6% ^{17}O isotope.

Acknowledgements

FVCK would like to thank the Brazilian agency FAPESP (Proc. 2012/23169-8, 2015/16624-9, and 2018/16040-5) for financial support. FA was supported by the EU and co-financed by the European Regional Development Fund under the project GINOP-2.3.2–15–2016-00008.

Conflict of interest

The authors declare no conflict of interest.

Keywords: contrast agents · kinetics · lanthanides · ligands · MRI · relaxation · thermodynamic

[1] L. M. De León-Rodríguez, A. F. Martins, M. Pinho, N. Rofsky, A. D. Sherry, *J. Magn. Reson. Imaging* **2015**, *42*, 545 – 565.
[2] C. S. Bonnet, P. H. Fries, S. Crouzy, P. Delangle, *J. Phys. Chem. B* **2010**, *114*, 8770 – 8781.
[3] P. Caravan, J. J. Ellison, T. J. McMurry, R. B. Lauffer, *Chem. Rev.* **1999**, *99*, 2293 – 2352.

[4] A. S. Merbach, L. Helm, É. Tóth, *The Chemistry of Contrast Agents in Medical Magnetic Resonance Imaging*, Wiley, Chichester, **2013**.
[5] C. F. G. C. Geraldes, S. Laurent, *Contrast Media Mol. Imaging* **2009**, *4*, 1–23.
[6] S. Aime, M. Botta, M. Fasano, E. Terreno, *Chem. Soc. Rev.* **1998**, *27*, 19–29.
[7] S. Hajela, M. Botta, S. Giraudo, J. Xu, K. N. Raymond, S. Aime, *J. Am. Chem. Soc.* **2000**, *122*, 11228–11229.
[8] E. J. Werner, J. Kozhukh, M. Botta, E. G. Moore, S. Avedano, S. Aime, K. N. Raymond, *Inorg. Chem.* **2009**, *48*, 277–286.
[9] E. Gianolio, G. B. Giovenzana, D. Longo, I. Longo, I. Menegotto, S. Aime, *Chem. Eur. J.* **2007**, *13*, 5785–5797.
[10] E. Gianolio, C. Cabella, S. Colombo Serra, G. Valbusa, F. Arena, A. Maiocchi, L. Miragoli, F. Tedoldi, F. Uggeri, M. Visigalli, P. Bardini, S. Aime, *J. Biol. Inorg. Chem.* **2014**, *19*, 715–726.
[11] I. Mamedov, J. Engelmann, O. Eschenko, M. Beyerlein, N. K. Logothetis, *Chem. Commun.* **2012**, *48*, 2755–2757.
[12] L. Manzoni, L. Belvisi, D. Arosio, M. P. Bartolomeo, A. Bianchi, C. Brioschi, F. Buonsanti, C. Cabella, C. Casagrande, M. Civera, M. De Matteo, L. Fugazza, L. Lattuada, F. Maisano, L. Miragoli, C. Neira, M. Pilkington-Miksa, C. Scolastico, *ChemMedChem* **2012**, *7*, 1084–1093.
[13] E. Farkas, J. Nagel, B. P. Waldron, D. Parker, I. Tóth, E. Brücher, F. Rösch, Z. Baranyai, *Chem. Eur. J.* **2017**, *23*, 10358–10371.
[14] B. P. Waldron, D. Parker, C. Burchardt, D. S. Yufit, M. Zimny, F. Roesch, *Chem. Commun.* **2013**, *49*, 579–581.
[15] J.-P. Sinnes, J. Nagel, B. P. Waldron, T. Maina, B. A. Nock, R. K. Bergmann, M. Ullrich, J. Pietzsch, M. Bachmann, R. P. Baum, F. Rösch, *EJNMMI Research* **2019**, *9*, 48.
[16] J. Martinelli, G. Gugliotta, L. Tei, *Org. Lett.* **2012**, *14*, 716–719.
[17] S. Aime, L. Calabi, C. Cavallotti, E. Gianolio, G. B. Giovenzana, P. Losi, A. Maiocchi, G. Palmisano, M. Sisti, *Inorg. Chem.* **2004**, *43*, 7588–7590.
[18] Z. Baranyai, F. Uggeri, G. B. Giovenzana, A. Benyei, E. Brucher, S. Aime, *Chem. Eur. J.* **2009**, *15*, 1696–1705.
[19] Z. Baranyai, F. Uggeri, A. Maiocchi, G. B. Giovenzana, C. Cavallotti, A. Takács, I. Tóth, I. Bányai, A. Bényei, E. Brucher, S. Aime, *Eur. J. Inorg. Chem.* **2013**, 147–162.
[20] Z. Baranyai, D. D. Castelli, C. Platas-Iglesias, D. Esteban-Gomez, A. Bényei, L. Tei, M. Botta, *Inorg. Chem. Front.* **2020**, *7*, 795–803.
[21] A. Vágner, E. Gianolio, S. Aime, A. Maiocchi, I. Toth, Z. Baranyai, L. Tei, *Chem. Commun.* **2016**, *52*, 11235–11238.
[22] D. Delli Castelli, L. Tei, F. Carniato, S. Aime, M. Botta, *Chem. Commun.* **2018**, *54*, 2004–2007.
[23] L. Barcza, K. Mihályi, *Z. Phys. Chem.* **1977**, *104*, 199–212.
[24] M. Botta, *Eur. J. Inorg. Chem.* **2000**, 399–407.
[25] K. Micskei, L. Helm, E. Brucher, A. E. Merbach, *Inorg. Chem.* **1993**, *32*, 3844–3850.
[26] T. J. Swift, R. E. Connick, *J. Chem. Phys.* **1962**, *37*, 307–320.
[27] a) L. R. Tear, C. Carrera, E. Gianolio, S. Aime, *Chem. Eur. J.* **2020**, *26*, 6056–6063; b) D. Delli Castelli, M. C. Caligara, M. Botta, E. Terreno, S. Aime, *Inorg. Chem.* **2013**, *52*, 7130–7138; c) C. Platas-Iglesias, *Eur. J. Inorg. Chem.* **2012**, 2023–2033; d) S. Aime, M. Botta, Z. Garda, B. E. Kucera, G. Tircso, V. G. Young, M. Woods, *Inorg. Chem.* **2011**, *50*, 7955–7965.
[28] T. J. Clough, L. Jiang, K.-L. Wong, N. J. Long, *Nat. Commun.* **2019**, *10*, 1420.
[29] J. Wahsner, E. M. Gale, A. Rodríguez-Rodríguez, P. Caravan, *Chem. Rev.* **2019**, *119*, 957–1057.
[30] E. Brücher, G. Tircsó, Z. Baranyai, Z. Kovács, A. D. Sherry in *The Chemistry of Contrast Agents in Medical Magnetic Resonance Imaging* (Eds.: A. S. Merbach, L. Helm, E. Toth), Wiley, Chichester, **2013**, pp. 157–208.
[31] P. M. May, P. W. Linder, D. R. Williams, *J. Chem. Soc. Dalton Trans.* **1977**, 588–595.
[32] Z. Baranyai, Z. Palinkas, F. Uggeri, A. Maiocchi, S. Aime, E. Brucher, *Chem. Eur. J.* **2012**, *18*, 16426–16435.
[33] Z. Baranyai, E. Brucher, F. Uggeri, A. Maiocchi, I. Toth, M. Andrasi, A. Gaspar, L. Zekany, S. Aime, *Chem. Eur. J.* **2015**, *21*, 4789–4799.
[34] A. Barge, G. Cravotto, E. Gianolio, F. Fedeli, *Contrast Media Mol. Imaging* **2006**, *1*, 184–188.
[35] H. M. Irving, M. G. Miles, L. D. Pettit, *Anal. Chim. Acta* **1967**, *38*, 475–488.
[36] L. Zékány, I. Nagypál in *Computational Methods for the Determination of Formation Constants* (Ed.: D. J. Leget), Plenum Press, New York, **1985**, pp. 291–353.

Manuscript received: October 6, 2020
Revised manuscript received: November 3, 2020
Accepted manuscript online: November 13, 2020
Version of record online: ■■ ▮▮, 0000

FULL PAPER

MRI Contrast Agents

F. V. C. Kock, A. Forgács, N. Guidolin, R. Stefania, A. Vágner, E. Gianolio, S. Aime, Z. Baranyai**

■■ – ■■

[Gd(AAZTA)]⁻ Derivatives with *n*-Alkyl Acid Side Chains Show Improved Properties for their Application as MRI Contrast Agents

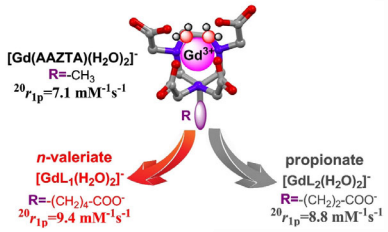

Bit on the side: The good properties of Gd(AAZTA) (AAZTA = 6-amino-6-methylperhydro-1,4-diazepine tetra acetic acid) as a MRI contrast agent are further improved by simply attaching a short *n*-alkyl function on the ligand's surface. The variable temperature (VT)-T_2 measurements of the $^{17}OH_2$ resonance suggest the occurrence of two interconverting isomers in solution characterized by very different exchange rates of the coordinated water molecules.

The good properties of Gd(AAZTA) as a MRI contrast agent are further improved by simply attaching a short n-alkyl function on the ligand's surface SPACE RESERVED FOR IMAGE AND LINK

Share your work on social media! *Chemistry - A European Journal* has added Twitter as a means to promote your article. Twitter is an online microblogging service that enables its users to send and read text-based messages of up to 140 characters, known as "tweets". Please check the pre-written tweet in the galley proofs for accuracy. Should you or your institute have a Twitter account, please let us know the appropriate username (i.e., @accountname), and we will do our best to include this information in the tweet. This tweet will be posted to the journal's Twitter account @ChemEurJ (follow us!) upon online publication of your article, and we recommended you to repost ("retweet") it to alert other researchers about your publication.

Please check that the ORCID identifiers listed below are correct. We encourage all authors to provide an ORCID identifier for each coauthor. ORCID is a registry that provides researchers with a unique digital identifier. Some funding agencies recommend or even require the inclusion of ORCID IDs in all published articles, and authors should consult their funding agency guidelines for details. Registration is easy and free; for further information, see http://orcid.org/.

Flávio Vinicius Crizóstomo Kock
Dr. Attila Forgács
Nicol Guidolin
Rachele Stefania
Dr. Adrienn Vágner
Dr. Eliana Gianolio
Prof. Silvio Aime
Dr. Zsolt Baranyai